CFD optimization of ATT flowmeters installed in short converging intakes of a pump station

Peng Zhang[1], Heming Hu[2], Jingqiao Mao[1], Qisen Miao[1], Yiqing Gong[1], Yunyu Tong[2]

[1] College of Water Conservancy and Hydropower Engineering, Hohai University, Nanjing, China
[2] National Institute of Metrology, Beijing, China
E-mail (corresponding author): jingqm@163.com

Abstract

The acoustic transit-time (ATT) method is a practical technique for online flow rate measurement. It is suitable for straight pipes, open channels, and even short converging intakes of pump stations. Some effective integration algorithms have been proposed and adopted for flow calculation in pipes and open channels, but further improvements are required for flow in short converging intakes due to their complex geometry. The Qianliulin pump station is the third stage of the cascade pump stations of Miyun Reservoir Regulation and Storage Project for the South to North Water Transfer Project of China. ATT flowmeters were installed in the short converging intakes of the pump station to measure the flow rates; each has the configuration of the double-plane with 4 paths each (i.e., the 8-path configuration). The tool of computational fluid dynamics (CFD) is used to investigate the accuracy of the ATT flowmeters installed in short converging intakes of the pump station. This paper mainly presents the numerical study on the complex flow field of the measuring section. Considering that the flow in the measuring section is sensitive to the fore bay structure, the approach channel and the elbow-shaped culverts are also included in the computational domain. The effects of the flow field on the metering performance under different operating conditions are analysed, and the systematic deviations are evaluated. Further discussion is also made for quantifying the effects of the integration algorithm and the path angle on the calculation of standard flow rates. This study can help optimize the flow rate integration algorithm.

1. Introduction

Water diversion projects, such as the South-to-North Water Diversion Project in China, are increasingly being constructed due to the unequal distribution of water resources among different regions. For such great water diversion projects, flow rate measurement is a key issue to determine the total discharge. The acoustic transit-time (ATT) method is a practical method for online flow rate measurement [1]. Flow rate is measured by transmitting and receiving acoustic signals diagonally across the water flow. It should be noted that the flow integration algorithm must be compatible with the installation condition. Routine flow integration algorithms are widely used and well verified for straight pipelines and open channels. However, for a variable-cross section tube, such as a short converging intake of a pump station, the variable-section domain needs to be converted to a rectangular pipe before employing the routine algorithms. The accuracy loss of the result should be evaluated and controlled caused by the domain conversion.

The Qianliulin pump station is the third stage of the cascade pump stations of Miyun Reservoir Regulation and Storage Project for the South to North Water Transfer Project. ATT flowmeters were installed in its short converging intakes to measure the flow rates. The flow measurement system adopts an 8-path configuration, i.e., 2 crossed acoustic planes with 4 paths each. That is, there are 16 probes installed on the both sides of the converging culvert. The cross section of the culvert is rectangular, but varying along the flow direction (a reducing trend of the cross section), namely the bottom face and the top face are not parallel, which brings a challenge for the calculation of flow rate based on the ATT flowmeters.

A more complete three-dimensional description of the culvert flow can be acquired from computational fluid dynamics (CFD) models [2-5]. Adequate details of the flow field are critical to optimize the flow rate integration algorithm and to evaluate the installation effects [3]. In this paper, a refined CFD model is used to simulate the flow field of converging intakes of the pump station, in which the multi-path ATT flowmeters were installed. By comparing with the actual measured data, the systematic deviations of conventional integration algorithms are quantified. The influence of the flow field on the performance of the flowmeters under different operating conditions is also analysed, and the standard flow rates using different integration algorithms are discussed.

2. Model set-up

Four vertical axial-flow pumps have been installed in the Qianliulin pump station. In order to monitor the flow rate of the pump station, a multi-path ultrasonic flow measurement system with ATT flowmeters was installed in the 4 short converging intakes, as shown in Figure 1.

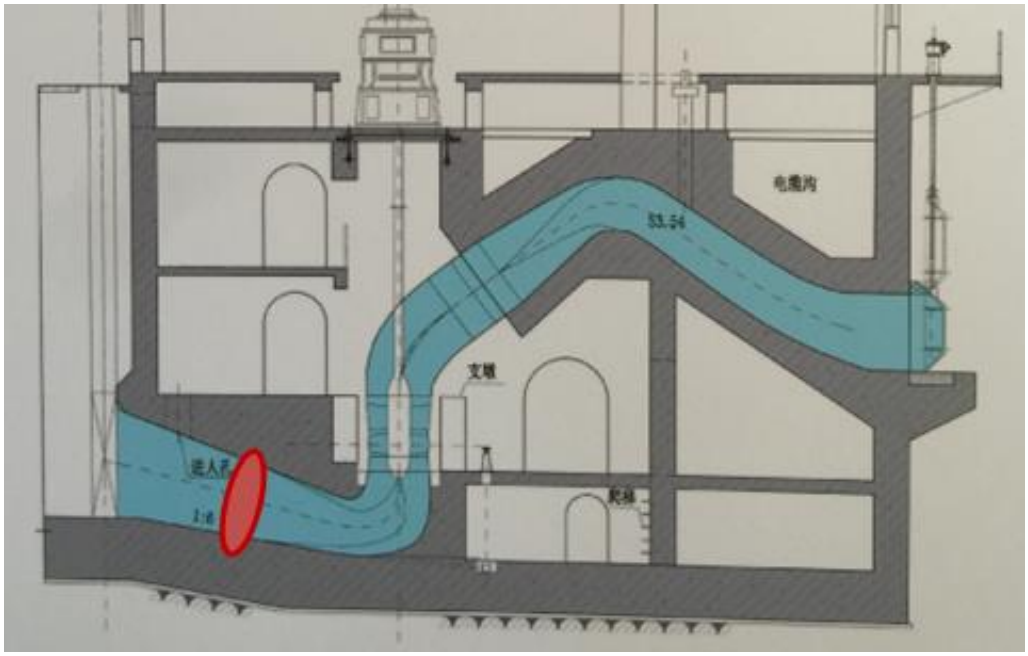

Figure 1: Installation position of the ATT flowmeters.

The geometric model of the intake part of the Qianliulin pump station is established by using the Solidworks 3D modeling software. The flow regime in the measuring section is sensitive to the fore bay structure, due to the drastic change of the upper channel section at the junction with the fore bay. Therefore, the inlet (upstream boundary) is set far enough away from the entrance of intakes. As such, the computational domain is composed of the approach channel, the fore bay, and the 4 short converging intakes as well as their elbow-shaped culverts (Figure 2).

The governing equations are the continuity equation and the Reynolds averaged Navier-Stokes equations. The realizable k-ε turbulent model is adopted to close the equation system. The software Fluent is used herein to simulate the flow field. The governing equations are discretized by the finite volume method, using a second-order implicit scheme in time, a second-order central difference scheme for the diffusion terms, and a second-order upwind scheme for the convection terms. The SIMPLEC method is used to solve the velocity-pressure coupling problem. The convergence criterion of numerical simulation is set as 10^4.

Almost seven billion structured grids are used to construct the grid system in the computational domain. In particular, locally refined grids are applied for accurate approximation of the regions around walls. The whole computational domain can be divided into 6 parts: the diversion channels part, the fore bay and 4 converging intakes (Figure 2). Boundary conditions must be applied at the bottom, water surface, vertical walls, inflow section and outflow section. The section of diversion river is taken as the entrance of the whole computational domain. The mean velocity of the section is fixed at 1 m/s. The water depth is 1.65 m under the design condition. At the water surface, the rigid-lid assumption is adopted. It implies that the free water surface is treated as a surface of symmetry for all variables. The outlet is located at the installation section of water pump blade, which is set as the pressure outlet (the relative pressure = 0). The rest boundaries are set as wall and treated with standard wall function.

2.2 Subsection headings

All second-level headings are numbered and in Times New Roman 10 point italic font. There should be a one-line space ahead of the heading and no space after the heading. The geometric model of the intake part of the Qianliulin pump station is established by using the Solidworks 3D modelling software. The flow regime in the measuring section is sensitive to the fore bay structure, due to the drastic change of the upper channel section at the junction with the fore bay. Therefore, the inlet (upstream boundary) is set far enough away from the entrance of intakes. As such, the computational domain is composed of the approach channel, the fore bay, and the 4 short converging intakes as well as their elbow-shaped culverts (Figure 2).

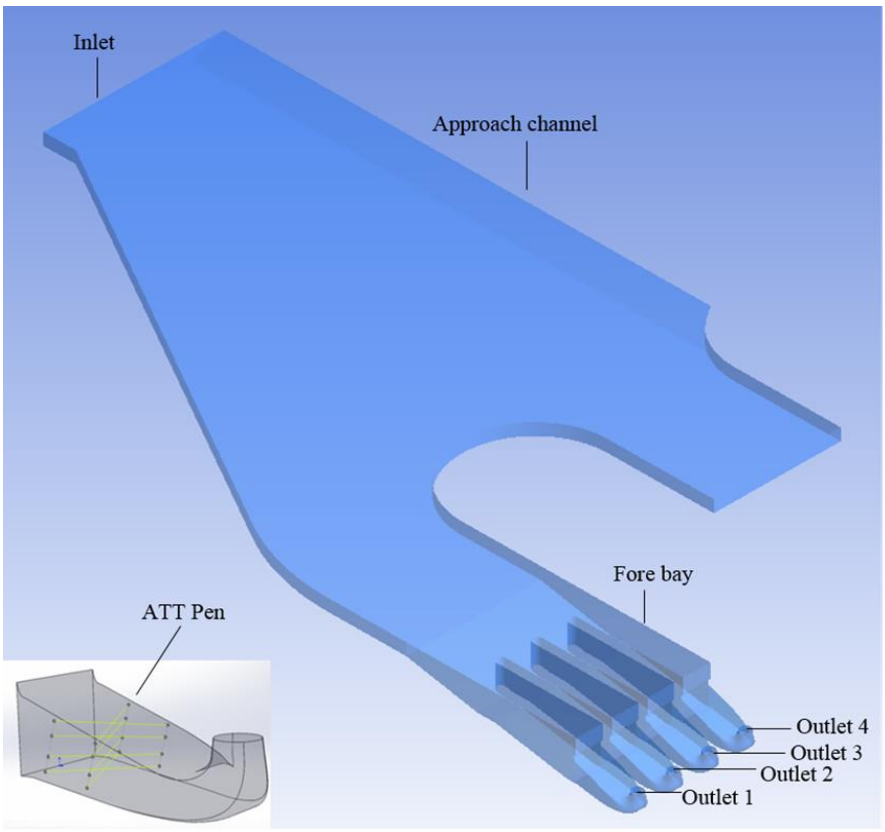

Figure 2: Sketch of the computational domain within the Qianliulin pump station.

.

3. Numerical simulation results

3.1 The approach channel

In order to understand the flow patterns of the open channel and the fore bay and the culverts, Figure 3 presents the three-dimensional streamlines of the computational domain.

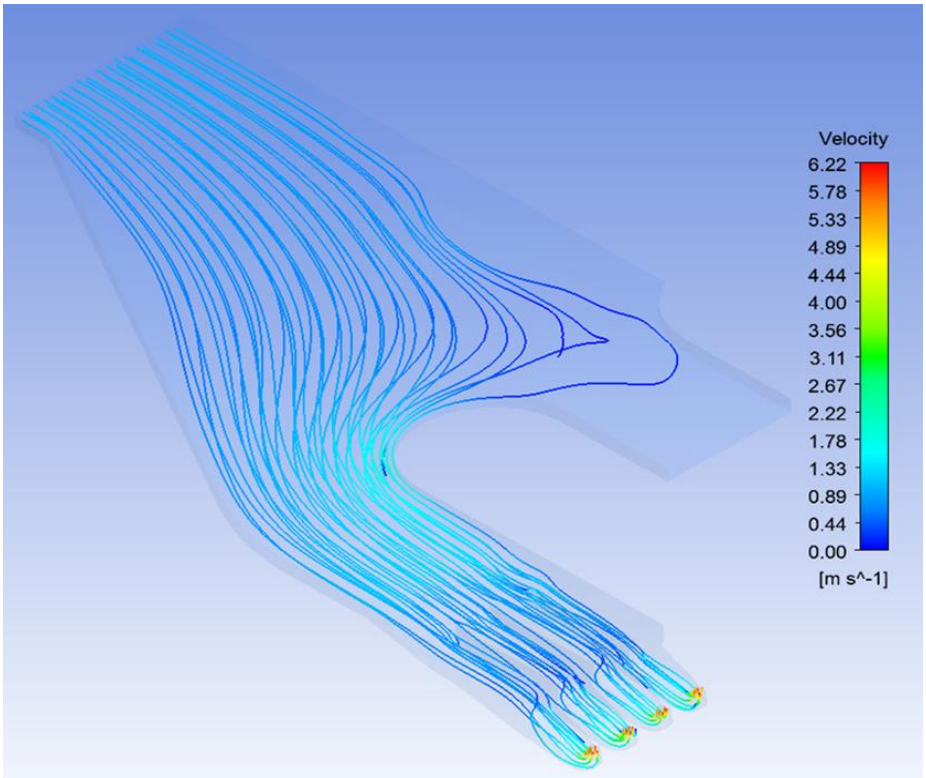

Figure 3: The three-dimensional streamlines of the simulation domain.

Under the restriction of the side walls, the mainstream flows to the fore bay. With the increasing of cross section areas, the velocity of the mainstream flow decreases. The mainstream is then squeezed in front of the side entrance, resulting in the reflux zone and backwater zone. The vortex can be observed near the gate (Figure 4).

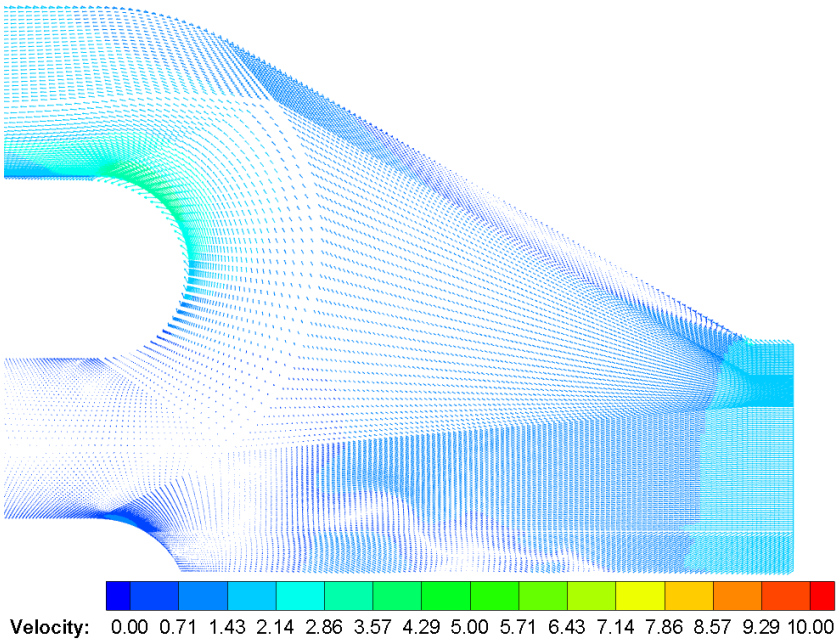

Figure 4: Velocity distribution in the approach channel.

3.2 The side entrance

As the cross-sectional area decreases and the velocity increases, the centrifugal force is formed as the result of the combination of the inertia, gravity and the roughness of the side wall; and, under the combined effects of centrifugal force and the walls, the flow direction changes several times.

When the mainstream fluid flows around the bend, because of the outward centrifugal force and the restraint of the walls, lateral water pressure increases whereas the inner pressure decreases, and lateral velocity decreases and the inside velocity increases accordingly. Therefore, there is a diffusion trend in the lateral curve and a shrinking trend in the inside curve. When the mainstream fluid flows out of the curve forward to the fore bay, the situation is opposite. The diffusion trend results in the flow off the side wall and the formation of vortex zone. The inertia of the flow in the curve can strengthen this effect, leading to the offset of the mainstream flow.

The presence of flow separation results in a significant reduction of the cross section of the fore bay and causes uneven velocity distribution in the longitudinal direction.

3.3 The fore bay

The fore bay is divided into 4 channels by 3 separate piers. Due to the deflection of the upstream flow in the bends, there is a transverse flow; the three piers may reduce the flow area, increase the velocity, prevent the offset of the mainstream flow, and improve the flow pattern in some conditions (Figure 5).

The offset of the mainstream flow can cause the uneven flow distribution in the left and right sides of channels. In general, the flow in the left side is shifted to the right side of the channel, the flow in the right is shifted to the left of the channel, and the flow in the middle channels is evenly distributed.

Because of the blocking of the solid wall, the flow produces backflow at two right angles at the top of each flow channel and thus has the vortex in the upper connection of the fore bay and the inlets of intakes.

3.4 The converging intakes and elbow-shaped culverts

As a result of the bias mainstream flow, unevenly distributed flow occurs on both sides of the channel. Because the right side of the fluid flows to the left, the flow in the inlet of the intake deflects to the right. The solid walls cause a bias in the flow direction and produce secondary flow in the horizontal section. The spiral flow is to be considered as the result of the combination of mainstream and secondary flows. As the cross section decreases, the flow pattern has to be adjusted, and the pressure and velocity tend to be distributed uniformly. The change of flow in the two-sided intakes are similar. For the middle intakes, the pressure and velocity distributions are more symmetrical.

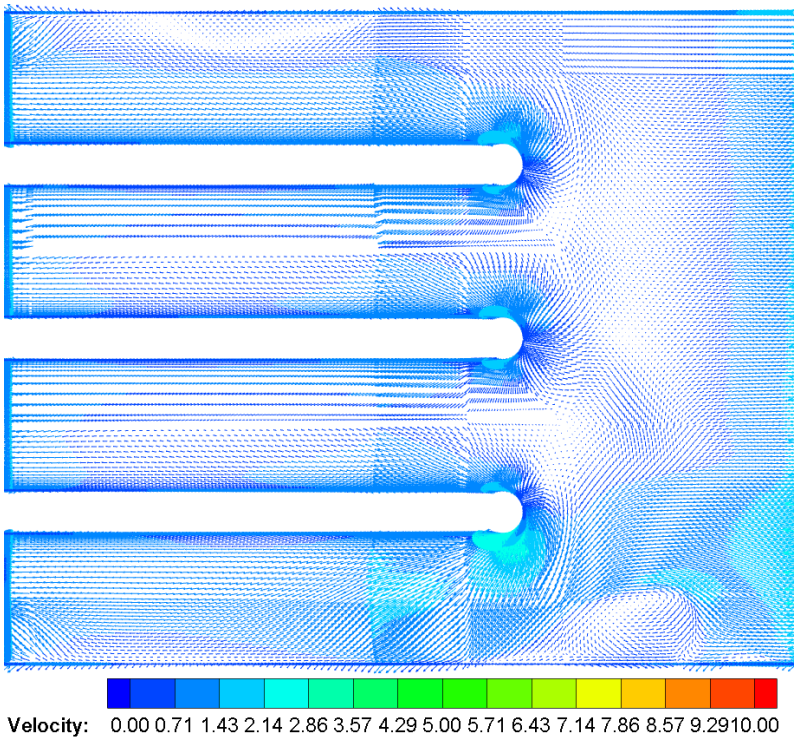

Figure 5: Velocity distribution in the fore bay.

In the transition of the straight rectangular section to the circular section, the flow turns 90 degrees. Under centrifugal force, the pressure of inner elbow is low and the velocity is high. There is a low-pressure area along the elbow's inner circle. But, due to the decrease of elbowed section, there is no bad flow (e.g., flow separation). The pressure is high and the velocity is low beyond the elbow. Due to the change of shape and the influence of centrifugal force, the flow velocity and pressure distributions are severely adjusted (Figure 6).

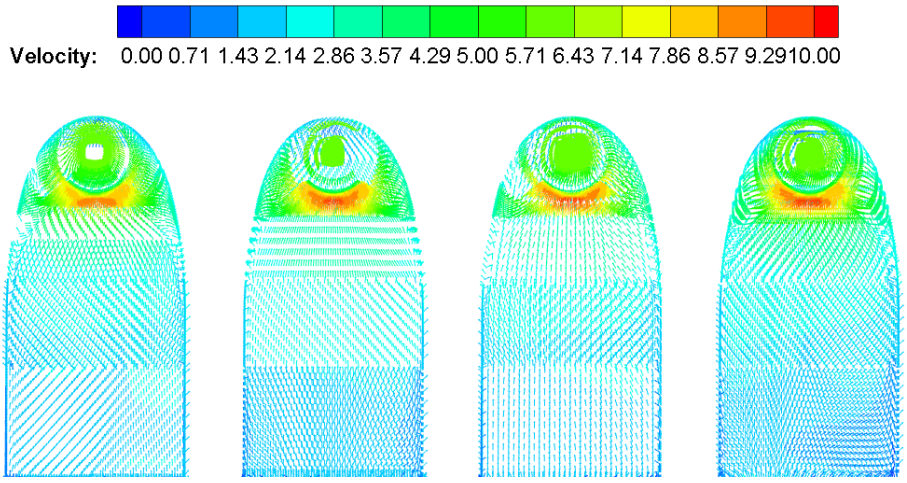

Figure 6: Velocity distribution in the elbow-shaped culverts.

4. Flow rate calculation

Installation effect is the possible flow error due to disturbed flow filed. The indication flow rate and standard flow rate are needed to calculate the flow errors caused by installation effect [3]. The indicated flow rate can be obtained by weighted averaging of path velocities based on the numerical flow filed along each acoustic path.

4.1 Calculation of indication flow rate

For the measurements, the projection velocity v_{proj} is determined from the transit time differences of the upstream and downstream acoustic pulses. The mean axial flow velocity of the path can be calculated via the angle of the path. Two methods are firstly introduced compute the indication flow rate; the main difference between them lies in the computational approach for v_{proj}.

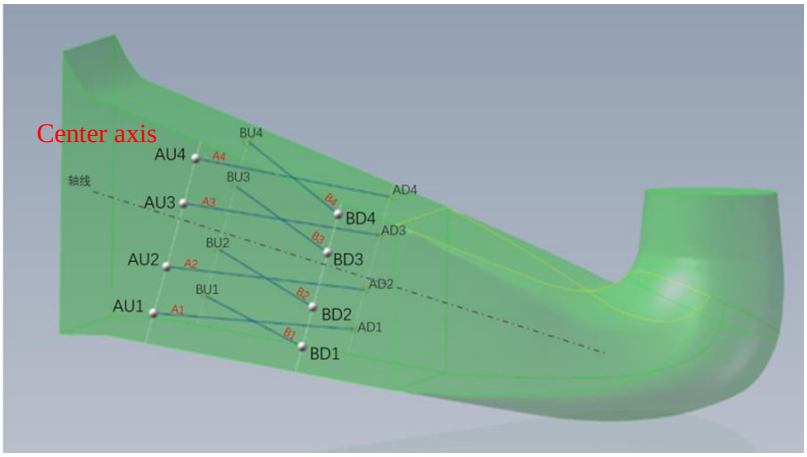

Figure 7: Path positions within the converging intake.

The general procedure to calculate the indication flow rate is given as flows:

(1) Extraction of the geometrical information (*x*, *y*, *z* co-ordinates) and the corresponding velocity components (*u*, *v*, *w*) of each path.

(2) Calculation of the mean velocities of each component (*u*, *v*, *w*) with the trapezoidal rule.

(3) Calculation of the axial velocity component v_{ax} along the axial flow direction, and the transversal velocity component v_{trans} normal to the axial flow direction.

(4) Calculation of v_{ax_proj} and v_{cross}:

$$v_{ax\_proj} = v_x \cdot \cos(\varphi) \quad (1)$$

$$v_{cross} = v_z \cdot \sin(\varphi) \quad (2)$$

(5) Calculation of v_{proj}

$$\text{Plane A: } v_{proj\_A} = v_{ax\_proj} + v_{cross} \quad (3)$$

$$\text{Plane B: } v_{proj\_B} = v_{ax\_proj} - v_{cross} \quad (4)$$

(6) Calculation of v_{ax}

$$\text{Plane A: } v_{ax\_A} = v_{proj} / \cos(\varphi) \quad (5)$$

$$\text{Plane B: } v_{ax\_B} = v_{proj} / \cos(\varphi) \quad (6)$$

(7) Calculation of $v_{ax\text{-}mean}$

Because of the uneven distribution of the nodes on the channel lines, and because we need to obtain the mean velocity of the channel lines, nodes are fitted by the trapezoidal rule.

(8) Calculation of v_{axial_l}

$$\tan\lambda_l = \frac{1-(v_{ax\_A}/v_{ax\_B})}{\tan\varphi_A + (v_{ax\_A}/v_{ax\_B}).\tan\varphi_B} \quad (7)$$

$$v_{axial,l} = 0.5 \cdot (v_A \cdot \frac{1}{1 - \tan\varphi \cdot \tan\lambda_l} + v_B \cdot \frac{1}{1 + \tan\varphi \cdot \tan\lambda_l}) \quad (8)$$

(9) Calculation of v_{cross_l}

$$v_{cross\_l} = v_{axial\_l} \cdot \tan\lambda_l \quad (9)$$

(10) Calculation of Q

For the rectangular flow path, the flow rate is usually calculated by Gauss-Legendre integration method and rectangular optimization integration method (OWIRS).

$$Q = \frac{BH}{2} \cdot \sum_{i=1}^{N} w_i \cdot V_i \quad (10)$$

The other method to calculate $v_{proj.}$ is to use the dot product method. Line averaged velocity vector vi and acoustic path velocity $v_{proj.}$ share the same projection on the corresponding acoustic path. Thus, v_{proj} can be expressed using dot products as follows,

$$v_{proj} = \left(\vec{v}_i \cdot \vec{l}\right) / \left(\vec{f} \cdot \vec{l}\right) \quad (11)$$

where flow unit vector $\vec{f} = (f_1, f_2, f_3)$ is mainstream direction; path unit vector $\vec{l} = \left(l_1, l_2, l_3\right)$ is from upstream transducer to downstream transducer.

Therefore, the most important thing is to obtain the line average flow rate on the channel line. The position of the channel line is determined by the coordinates of both ends. The scatter velocity in three-dimensional flow field can be interpolated to the channel line; since the nodes on the channel line are not equal to each other, the average velocity of the line is not the arithmetic average of the velocity of each node, but it needs to be calculated by the formula and the line integral. The PCHIP method is adopted in the fitting process, which avoids the problem of local overvaluation or underestimation caused by linear fitting.

4.2 Calculation of standard flow rate

FLUENT can directly provide the flow rate at a certain section by the built-in integration algorithm. In this section, we briefly compare the calculated indication flow rates and the standard flow rates given by FLUENT. In Table 1, the deviation 1 means the error between the indication flow rate 1 and the standard flow rate; the deviation 2 means the error between the indication flow rate 2 and the standard flow rate.

Table 1 Comparison of flow rates (m^3/s) and deviations

	Intake 1	**Intake 2**	**Intake 3**	**Intake 4**
Standard flow rate	9.151081	9.159491	9.090051	9.009708
Indication flow rate 1	8.428355208	8.399345108	8.302570938	8.299416513
Deviation 1	7.89%	8.29%	8.66%	8.18%
Indication flow rate 2	8.6673641	8.671708686	8.545200751	8.512635795
Deviation 2	5.28%	5.32%	5.99%	5.51%

It is shown that the indication flow rates from we obtain from two kinds of algorithms are approximately equal to the standard flow rate directly given by FLUENT, and the deviation is generally less than 9%. However, the deviations between them are significant, which should be discussed further.

5. Discussion

5.1 Choice of standard flow rate

The standard flow rate is the product of the area and the area-averaged velocity of the cross section. Although Fluent may provide the flow rate at a certain section, the most reliable method may be the integration base on triangulation [3]. As such, we extract all the node velocities of measuring section from the numerical flow field, and then establish triangular

grids using Delaunay Triangulation method (Figure 8). The axial velocity for each grid is the average value of velocities at three fixed points of the triangle. The standard flow rate is the sum of flow rates on all triangular grids.

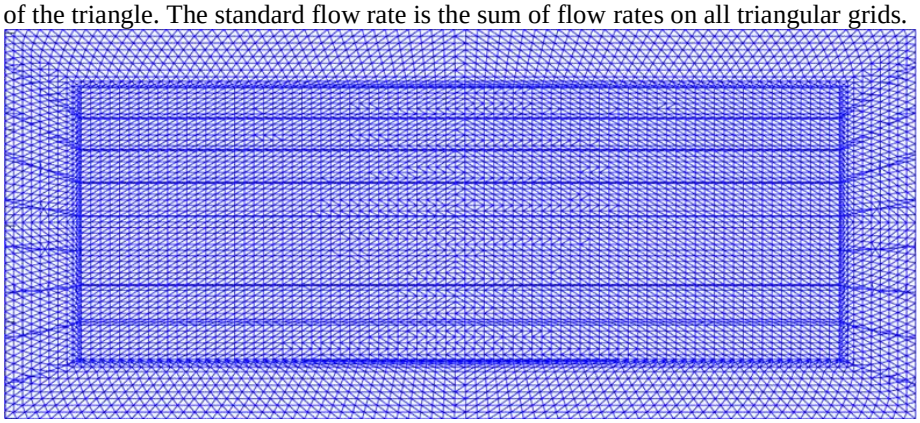

Figure 8: Integration base on Delaunay Triangulation.

If adequate acoustic paths can be applied in the numerical flow fields to calculate the indication flow rate, which should be the same as the actual flow rate if the truncation error is small enough. Figure 9 compares the calculated flow rates from the Delaunay Triangulation method (8.93 m^3/s), Fluent (9.15 m^3/s), and Gauss integration method with increasing path number (9.02 m^3/s from the case of 20-path). With the increasing of path numbers, the calculated flow rates tend to be close to the results of the other two methods. In particular, the relative difference between the Delaunay Triangulation method and the Gauss integration method is smaller (~0.79% with increasing path number). It is clear that at least 7 acoustic paths are good enough to produce the calculated flow rate that can be regarded as the standard flow rate.

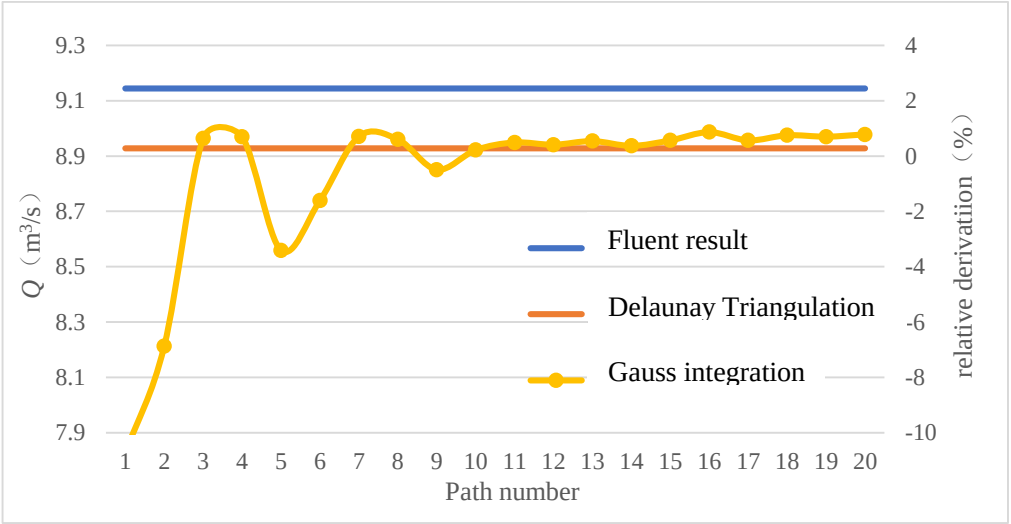

Figure 9: The calculated flow rates and the relative difference.

5.2 Effect of path angles

An acoustic path angle refers to the intersection angle between the acoustic path and the axial line of an intake. There are two different path angles (53 °and 65 °) for the ATT flowmeters installed in the intakes of the Qianliulin pump station. We calculated the flow rates with different path angles in the 4 intakes, which are compared to the standard flow rates given by the Gauss integration method (20 paths). Table 2 and 3 present the results using the adjusted and standard weighting coefficients, respectively. It is interesting to note that, there is no significant difference between the calculated indication flow rates with different path angles (~1%).

Table 2 Calculated flow rates with different path angles (adjusted weighting coefficients)

	Intake 1	**Intake 2**	**Intake 3**	**Intake 4**
20-path flow rate (m^3/s)	9.02	9.05	8.96	8.89
Path angle 53° (m^3/s)	8.74	8.75	8.72	8.60
Relative difference 1	-3.10%	-3.31%	-2.68%	-3.26%
Path angle 65° (m^3/s)	8.68	8.75	8.67	8.49
Relative difference 2	-3.77%	-3.31%	-3.24%	-4.50%
Relative difference between 2 angles	-0.69%	0	-0.57%	-1.28%

Table 3 Calculated flow rates with different path angles (standard weighting coefficients)

	Intake 1	**Intake 2**	**Intake 3**	**Intake 4**
20-path flow rate (m^3/s)	9.02	9.05	8.96	8.89
Path angle 53° (m^3/s)	9.24	9.25	9.23	9.08
Relative difference 1	2.44%	2.21%	3.01%	2.14%
Path angle 65° (m^3/s)	9.17	9.25	9.18	8.98
Relative difference 2	1.66%	2.21%	3.01%	1.01%
Relative difference between 2 angles	-0.76%	0	-0.54%	1.10%

All mathematical variables must be clearly defined. The equation should be centred in the column using a 4 cm centre tab, and the equation number should be parenthesised and located at the 8 cm edge of the text column using the right-hand tab.

6. Conclusion

The precision of ATT has a close relation with flow conditions. This paper presents the numerical study on the flow field of the measuring intakes based on a CFD model. The effect of flow field on the metering performance under different operating conditions is analysed, and the systematic deviations are evaluated. We further discuss the choice of standard flow rates using different integration algorithms, as well as the effect of path angles. This study can help optimize the flow rate integration algorithm.

References

[1] JJG1030-2007: *Ultrasonic flowmeters*, National verification regulation, 2007.

[2] Hug, Silvan, Thomas Staubli, and Peter Gruber. “Comparison of measured path velocities with numerical simulations for heavily disturbed velocity distributions.” 9th IGHEM. 2012.

[3] HM Hu, L Zhang, T Meng, C Wang. “Mechanism analysis and estimation tool of installation effect on multipath ultrasonic flowmeter.” 9th ISFFM.2015

[4] Marushchenko, S., P. Gruber, and T. Staubli. "Approach for acoustic transit time flow measurement in sections of varying shape: Theoretical fundamentals and implementation in practice." Flow Measurement and Instrumentation, 49, pp.8-17. 2016

[5] C Wang, T Meng, HM Hu, and L Zhang. "Accuracy of the ultrasonic flow meter used in the hydroturbine intake penstock of the Three Gorges Power Station." Flow Measurement and Instrumentation 25, pp. 32-39. 2012